Naval Surface Warfare Center
Carderock Division
West Bethesda, MD 20817-5700

NSWCCD-50-TR–2002/053 November 2002

Hydromechanics Directorate

Technical Report

Scaling of Noise Generation
Due to a Single Bubble in a Cavitating Trailing Vortex

by

Y. T. Shen

G. L. Chahine

C-T. Hsiao

S. D. Jessup

20030213 089

REPORT DOCUMENTATION PAGE

Public reporting burden for this collection of information is estimated to average 1 hour per response, including the time for reviewing instructions, searching existing data sources, gathering and maintaining the data needed, and completing and reviewing this collection of information. Send comments regarding this burden estimate or any other aspect of this collection of information, including suggestions for reducing this burden to Department of Defense, Washington Headquarters Services, Directorate for Information Operations and Reports (0704-0188), 1215 Jefferson Davis Highway, Suite 1204, Arlington, VA 22202-4302. Respondents should be aware that notwithstanding any other provision of law, no person shall be subject to any penalty for failing to comply with a collection of information if it does not display a currently valid OMB control number. **PLEASE DO NOT RETURN YOUR FORM TO THE ABOVE ADDRESS.**

1. REPORT DATE (DD-MM-YYYY) 1-Nov-2002	2. REPORT TYPE Final	3. DATES COVERED (From - To) 1-Oct-2001 – 1-Oct-2002

4. TITLE AND SUBTITLE	5a. CONTRACT NUMBER
Scaling of Noise Generation Due to a Single Bubble in a Cavitating Trailing Vortex	5b. GRANT NUMBER
	5c. PROGRAM ELEMENT NUMBER

6. AUTHOR(S)	5d. PROJECT NUMBER
Y. T. Shen, G. L. Chahine,* C-T. Hsiao,* and S. D. Jessup	5e. TASK NUMBER
* Dynaflow Inc., 10621-J Iron Bridge Rd, Jessup MD 20794	5f. WORK UNIT NUMBER 02-1-5080: 218-52 and 228-69

7. PERFORMING ORGANIZATION NAME(S) AND ADDRESS(ES) AND ADDRESS(ES)	8. PERFORMING ORGANIZATION REPORT NUMBER
Naval Surface Warfare Center Carderock Division 9500 Macarthur Boulevard West Bethesda, MD 20817-5700	NSWCCD-50-TR-2002/053

9. SPONSORING / MONITORING AGENCY NAME(S) AND ADDRESS(ES)	10. SPONSOR/MONITOR'S ACRONYM(S)
NAVSEA 93R, Doug Dahmer and NSWCCD Code 5080, Jude Brown	NAVSEA PMS 450, Larry Becker and NSWCCD Code 5080, Jack Lee
	11. SPONSOR/MONITOR'S REPORT NUMBER(S)

12. DISTRIBUTION / AVAILABILITY STATEMENT
Approved for public release; distibution is unlimited.

13. SUPPLEMENTARY NOTES

14. ABSTRACT
Scaling of noise generation due to a single bubble in a cavitating trailing vortex is studied. Vortex core dynamics between full-scale and model is mathematically formulated based on a similarity flow approach and McCormick's hypothesis. Acoustic frequency and amplitude scaling formulas to obtain full-scale acoustic spectrum from model data are derived. The acoustic scaling formulas are also compared with bubble dynamic calculations with encouraging results. The numerical calculations are obtained from a Dynaflow Inc. computer code. The acoustic scaling formulas are compared with Strasberg's classic lambda scaling and noise level scaling.

15. SUBJECT TERMS
Acoustic Spectrum Scaling, Cavitation, Trailing Vortex Cavitation

16. SECURITY CLASSIFICATION OF:			17. LIMITATION OF ABSTRACT	18. NUMBER OF PAGES	19a. NAME OF RESPONSIBLE PERSON Y. T. Shen
a. REPORT UNCLASSIFIED	b. ABSTRACT UNCLASSIFIED	c. THIS PAGE UNCLASSIFIED	SAR	vi+27	19b. TELEPHONE NUMBER (include area code) 301-227-1411

i

This page was intentionally left blank.

CONTENTS

FIGURES

NOTATION

The notations used in this document are consistent with the International Towing Tank Conference ITTC Standard Symbols from the "International Towing Tank Conference ITTC Symbols and Terminology List, Final Version 1996." Prepared by the 21st ITTC Symbols and Terminology Group; Edited and Produced by Bruce Johnson, U. S. Naval Academy, Annapolis, MD 21402-5042, USA.

a_c	Vortex core radius
c	Blade chord length
C_p	Pressure coefficient
D	Propeller diameter
f_p	Frequency at the peak amplitude of a noise spectrum
g	Acceleration due to gravity
h	Depth of submergence
J	Propeller advance coefficient
L	Radiated noise level
p(R)	Local pressure in the trailing vortex
P_∞	Reference (Ambient) pressure
Pa	Acoustic pressure
P_{atm}	Atmospheric Pressure
P_e	Encounter pressure
p_g	Gas pressure inside a bubble
p_v	Vapor pressure of the fluid
n	Exponent used in Reynolds scale formula for cavitation inception
N	Number of cavitation events per unit time
r	Radial distance from the vortex core center
R	Time dependent bubble radius
R_0	Initial bubble radius
Rp	Propeller radius
Re	Reynolds number based on the chord length
s	Acoustic amplitude spectrum
S	Surface tension of the fluid
t	Time
T_c	Total time of collapse
$\bar{U} - \bar{U}_b$	Slip velocity between the fluid and the bubble
V_∞	Reference velocity
V_t	Tangential velocity of the trailing vortex

NOTATION - Continued

α	Angle of attack
Γ	Circulation along the vortex core
ρ	Fluid density
$\flat$	Peak acoustic pressure
σ	Cavitation number
σ_i	Cavitation inception number
γ	Bound vortex on the blade surface
λ	Linear scale ratio between full-scale and model scale
υ	Volume of the bubble
μ	Dynamic viscosity

SUBSCRIPTS

f	Full-scale
m	Model
max	Maximum
min	Minimum

ENGLISH TO METRIC CONVERSIONS

1 degree (angle)	=	0.01745 rad (radians)
1 ft (foot)	=	0.3048 m (meters)
1 ft/s (foot per second)	=	0.3048 m/s (meters per second)
1 in (inch)	=	25.40 mm (millimeters)
1 knot	=	0.5144 m/s (meters per second)
1 lbf (pound-force)	=	4.448 N (newton)
1 lbf-in (pound-force-inch)	=	0.1130 N-m (newton-meters)
1 long ton (2240 pounds)	=	1.016 metric tons or 1016 kg (kilograms)
1 hp (horsepower)	=	0.746 kW (kilowatts)

ABSTRACT

Scaling of noise generation due to a single bubble in a cavitating trailing vortex is studied. Vortex core dynamics between full-scale and model is mathematically formulated based on a similarity flow approach and McCormick's hypothesis. Acoustic frequency and amplitude scaling formulas to obtain full-scale acoustic spectrum from model data are derived. The acoustic scaling formulas are also compared with bubble dynamic calculations with encouraging results. The numerical calculations are obtained from a Dynaflow Inc. computer code. The acoustic scaling formulas are compared with Strasberg's classic λ scaling and noise level scaling.

ADMINISTRATIVE INFORMATION

INTRODUCTION

A three-dimensional lifting surface has a vortex trailing from its tip caused by the crossover of fluid from the high-pressure side to the low pressure side. For propellers, the vortices from the blades form a helical path downstream of the blades. The vortices spin faster and cause regions of low pressure in their core at conditions of higher speeds or higher propeller thrust (loading). When the pressure in the core drops below the vapor pressure of the flowing liquid, cavitation can occur. On a marine propeller, cavitation typically occurs in the trailing vortex before it occurs on the blade surface. The prediction of the onset of tip vortex cavitation is of major interest to the Navy because of the noise and hull vibration associated with the vortex cavitation. The flow field in a trailing vortex is sufficient complex that prediction of cavitation inception and noise generation still relies heavily on model tests extrapolated to full-scale using cavitation scaling laws.

When a model propeller is tested, cavitation inception numbers σ_i with respect to different ship speeds and depths are determined. Acoustic signatures associated with various stages of cavitation are measured. Three scaling formulas are needed to translate model data to full-scale performance; (1) cavitation inception scale to predict cavitation inception speed of the full-scale propeller at a given depth or cavitation inception depth at a given speed, (2) frequency scaling of acoustic spectra, and (3) amplitude scaling of acoustic spectra. In this report, frequency scaling and amplitude scaling of noise generated by bubble cavitation are studied. The cavitation inception scaling has been formulated and presented by Shen et al [2001], [*] Shen, Jessup and Gowing, [2001], Hsiao, Chahine and Liu [2000] and Hsiao and Chahine [2002].

---

[*] References are listed in alphabetical order on page 25.

Cavitation noise and associated noise scaling has been studied by many researchers (see review papers by Strasberg [1977], Chahine [1979], Blake and Sevik [1982], Blake [1986] and Baiter [1982, 1989]). Due to complexity of the flow field in a tip vortex, the effect of pressure and vortex core dynamics on bubble cavitation and noise generation has not been considered. Experimental data indicate that tip vortex cavitation inception is sensitive to the Reynolds scale (McCormick [1954]) and free stream nuclei (Acosta and Parkin [1975]). Scaling of noise generation due to bubble cavitation in trailing vortices is studied in this report.

In the first part of this report, vortex core dynamics between full-scale and model is mathematically formulated. The scaling formulas to obtain full-scale acoustic spectrum form model data are derived. The present acoustic-scaling formulas are compared with Strasberg's classic λ scaling and noise level scaling. In the second part of this report, the present acoustic-scaling formulas are evaluated with bubble dynamic calculations. The numerical calculations are based on the modified Surface Averaged Pressure (SAP) Rayleigh-Plesset bubble dynamic equation (Hsiao et al [2002]). Bubble growth, collapse, and radiated noise due to a cavitation bubble are computed for a trailing vortex with prescribed circulation and pressure distributions along the vortex core.

PROBLEM FORMULATION AND SOLUTION APPROACH

To model the vortex and roll-up process, consider a propeller blade with a system of trailing vortices as shown in Figure 1. Let V_∞, and P_∞ denote the free stream velocity and reference pressure, γ the local bound vorticity on the foil. Let Rp and c denote the propeller radius and local chord length. Let Γ represent the vorticity in the trailing vortex, C_p is the pressure coefficient in the vortex core, and a_c is the radius of the vortex core.

Let λ denote the linear-scale geometric ratio of full-scale to model-scale, namely $Rp_f = \lambda Rp_m$ and $c_f = \lambda\, c_m$, where subscripts 'm' and 'f' denote the model and full-scale, respectively. Let J denote the propeller advance coefficient. In the scaling study, it is assumed that the advance coefficients are the same for full-scale propeller and model propeller. The hydrodynamic angle into the blade section will be the same for model and full-scale. Assuming both model and full-scale have the same planform, camber and section profiles, *geometric* similarity between the model and full-scale is preserved. For uniform inflow and same angles of attack on both propeller blade section, namely $\alpha_f = \alpha_m$, *kinematic* similarity is also satisfied. For dynamic similarity, it is assumed that the trailing edge vortex roll-up process between model and full-scale is similar. For simplicity a Rankine vortex model will be used to relate circulation, core dimension, tangential velocity and pressure distributions.

The process of bubbles' capture into the tip vortex is complex. In the present study it is assumed that a bubble enters the vortex core and convects downstream. The vortex core is a region of low pressure. For sufficiently low pressures, a bubble entering a vortex core will cavitate, experience growth and collapse, and radiate acoustically. It is presently assumed that the bubble remains spherical throughout the cavitation process. The cavitation spectrum covers a wide range of frequencies. The scaling of peak acoustic frequency and amplitude due to collapse of a single bubble in a trailing vortex is investigated here.

FREQUENCY AT PEAK AMPLITUDE DUE TO COLLAPSE OF A SPHERICAL BUBBLE

The behavior of a spherical bubble in a pressure field for incompressible flow is given by the Rayleigh equation (Plesset [1948], Fitzpatrick and Strasberg [1956])

$$R\,(d^2R/dt^2) + 3/2\,(dR/dt)^2 = 1/\rho\,(p_v + p_g - P_e - 2S/R) \equiv 1/\rho\,(p(R) - P_e),\qquad(1)$$

where $p(R) = p_v + p_g - 2S/R$ is the pressure in the liquid just outside the bubble surface. R is the time dependent bubble radius, ρ is the liquid density, p_v is the vapor pressure of the fluid, p_g is the gas pressure inside the bubble, P_e is the ambient pressure inside the vortex core local to the bubble, and S is the surface tension of the fluid. Under tension the bubble will grow as it is convected downstream inside the vortex core. In a high-pressure zone, the bubble will collapse. Before the collapse, the bubble attains a maximum bubble size, which is denoted by R_{max}. It is noted that $p(R) - P_e > 0$ when the bubble is in growing stage and, $p(R) - P_e < 0$ when the bubble is in collapsing stage. This fact is utilized in the following derivation.

For the collapse phase, Rayleigh found the total time of collapse T_c to be (Lamb [1945])

$$T_c = 0.915\,R_{max}\sqrt{\rho\big/(P_e - p(R))}\ ,\qquad(2)$$

where $P_e - p(R)$ are taken when $R = R_{max}$. Equation (2) is only approximate, since it does not take into account the fact that P_e is not always constant. Ross [1976] presented an idealized cavitation spectrum as shown in Figure 2 (also see Fitzpatrick and Strasberg [1956]). Measured cavitation spectra from analyzing the available experimental data show the peak amplitude occurring at a frequency related to the collapse time of the largest bubble;

$$f_p = \tfrac{1}{2}(1/R_{max})\sqrt{(p(R) - P_e)\big/\rho}\ ,\qquad(3)$$

aside from difference of constants, the frequency at peak amplitude in equation (3) gives the same expression as the Rayleigh bubble collapse time in equation (2) since a frequency is the inverse of time.

Let f_{pm} denotes the frequency at peak amplitude of the noise spectra generated by the model due to a bubble cavitation. Let the subscript m denote the variables associated with the model. We have:

$$f_{pm} = \tfrac{1}{2}(1/R_{max\,m})\sqrt{(p(R) - P_e)_m\big/\rho_m}\ .\qquad(4)$$

The Rayleigh bubble dynamic equation expressed in Equation (1) is quite general and is applicable model scale as well as full-scale. Let f_{pf} denote the peak frequency of the noise

3

spectra generated by the full-scale due to a bubble cavitation. Let the subscript f denote the variables associated with the full-scale. We have:

$$f_{pf} = \tfrac{1}{2}(1/R_{max\,f})\sqrt{(p(R)-P_e)_f/\rho_f}$$

(5)

From (4) and (5), we have:

$$f_{pf} = f_{pm}\left(\frac{R_{max\,m}}{R_{max\,f}}\right)\left(\frac{\sqrt{(p(R)-P_e)_f}}{\sqrt{(p(R)-P_e)_m}}\right)\left(\frac{\sqrt{\rho_m}}{\sqrt{\rho_f}}\right)$$

(6)

The frequency of the noise spectrum generated in full-scale due to collapse of a cavitation spherical bubble can be predicted from the model data by Equation (6). Note that the right hand side of Equation (6) is expressed in dynamic variables. To be useful for scaling, the dynamic variables must be expressed in terms of geometric and kinematic variables.

The Ratio of $R_{max\,m}$ / $R_{max\,f}$ in a Trailing Vortex: Experimental data indicate that tip vortex cavitation inception is very sensitive to Reynolds scaling. McCormick's experimental data [1954] show that cavitation inception is well represented by

$$\sigma_{if}\,/\,\sigma_{im} = (Re_f\,/\,Re_m)^n .$$

(7)

Shen, Jessup and Gowing [2001] have derived a theory for high Reynolds number application. Their theoretical result gives

$$n = \frac{5.16\,Log\,(Log\,Re_f/Log\,Re_m)}{Log\,(Re_f/Re_m)}$$

(8)

The numerical values of n as function of Reynolds numbers are given in Figures 3 and 4. The values of n decrease as the values of Reynolds number increase. For examples, n = 0.40, 0.33, and 0.31 at $Re = 3\times10^5$, 5×10^6, and 10^7, respectively.

Based on similarity flow approaches, Shen, Jessup and Gowing [2001] have theoretically derived the ratio of vortex core sizes in model and full-scale as

$$a_{cf}/\,a_{cm} = \lambda(Re_f\,/\,Re_m)^{-n/2},$$

(9)

where λ is the linear scale ratio of full-scale and model, Re_m and Re_f are model and full-scale Reynolds number, respectively. Equation (9) shows the viscous effects on the vortex core size. As to be shown later in the numerical section, the ratio of maximum bubble radii computed by Hsiao et al [2000] are related to the vortex core sizes as following

$$R_{max\,m}/\,a_{cm} = R_{max\,f}/\,a_{cf}.$$

(10)

4

In dimensional analysis for scaling, a variable must be expressed in a non-dimensional form. As a cavitation bubble is convected downstream inside the trailing vortex core, the pressure field in the vortex determines the growth and collapse of the bubble. For the pressure distributions inside a vortex core to be represented by a Rankine model, Equation (10) states that the characteristic length to normalize the maximum bubble radius is the vortex core size. From Equations (9) and (10), we have

$$R_{max\ m} / R_{max\ f} = (Re_f / Re_m)^{n/2} / \lambda . \tag{11}$$

The ratio of dynamic variables $R_{max\ m} / R_{max\ f}$ has now been expressed in geometric and kinematic variables.

The Ratio of $\sqrt{(P_e - p(R))_f} / \sqrt{(P_e - p(R))_m}$ *in a Trailing Vortex*: The pressure in a trailing vortex for a bubble to collapse is defined in Equation (1). At R= Rmax, the terms p_g and $2S/Rmax$ are small. Recall that P_e is the encounter pressure inside the vortex core local to the bubble at $R = R_{max}$. For a vaporous cavitation bubble, Equation (1) gives:

$$p(R) - P_e \approx p_v - P_e = p_v - P_\infty + P_\infty - P_e$$

$$= - (0.5\rho V_\infty^2) (C_p + \sigma) , \tag{12}$$

where $C_p \equiv (P_e - P_\infty) / (0.5\rho V_\infty^2)$ and $\sigma \equiv (P_\infty - p_v) / (0.5\rho V_\infty^2)$. $\tag{13}$

So

$$\sqrt{(p(R) - P_e)_f} / \sqrt{(p(R) - P_e)_m} = \sqrt{-(C_p + \sigma)_f} / \sqrt{-(C_p + \sigma)_m} (V_{\infty f} / V_{\infty m}) \tag{14}$$

where ρ_f / ρ_m has been set to equal 1.

Assume that cavitation inception occurs when the pressure in the core drops below the vapor pressure. We have:

$$\sigma_{if} / \sigma_{im} = C_{pminf} / C_{pminm} . \tag{15}$$

From a Rankine vortex model, Equations (12), (13) and (15) give

$$\sqrt{(p(R) - P_e)_f} / \sqrt{(p(R) - P_e)_m} = (Re_f / Re_m)^{n/2} (V_{\infty f} / V_{\infty m}) . \tag{16}$$

The ratio of dynamic variables

$$\sqrt{(p(R) - P_e)_f} / \sqrt{(p(R) - P_e)_m}$$

at $R = R_{max}$ has now been expressed in geometric and kinematic variables.

5

SCALING OF FREQUENCY AT PEAK AMPLITUDE

For $\rho_f/\rho_m = 1$, Equation (6) gives

$$f_{pf} = f_{pm}\left(\frac{R_{max\,m}}{R_{max\,f}}\right)\left(\frac{\sqrt{(p(R)-P_e)_f}}{\sqrt{(p(R)-P_e)_m}}\right) = f_{pm}\left(\frac{1}{\lambda}\right)\left(\frac{Re_f}{Re_m}\right)^n\left(\frac{V_{\infty f}}{V_{\infty m}}\right) \tag{17}$$

As shown in Equation (8), at very high Reynolds numbers, the value of n approaches zero. Only in this condition, Equation (17) gives the same result as Strasberg's well-known λ frequency scaling [1957, 1977] if viscous flow effects are neglected. Namely, Equation (17) provides tip vortex Reynolds number correction to Strasberg's λ frequency scaling.

Effect of Free Stream Nuclei Size on Frequency Scaling: As shown in Equation (1), when a bubble is in a static equilibrium, the balance of pressure across the bubble interface can be written:

$$P_e = p_v + p_g - 2S/R . \tag{18}$$

The bubble becomes unstable and experiences rapid growth when the derivative of pressure gradient, $dP/dR > 0$. Because of the intrinsic property of bubble dynamics, at a given cavitation number, a bubble grows to about the same maximum size regardless of the initial bubble sizes (Chahine and Shen [1986], Strasberg [1957]). The frequency scaling given in Equation (17) should not be affected by free stream nuclei size distributions as long as the cavitation noise is generated by non-interacting bubbles.

SCALING OF ACOUSTIC AMPLITUDE

Acoustic pressure: The relation between the radial motion of a growing and collapsing cavity and the pressure in the surrounding liquid have been treated extensively in the literature relating to cavitation and underwater explosion (see Strasberg [1956], Fitzpatrick [1958]). For incompressible flow we have (Fitzpatrick [1958]):

$$p(r,t) - P_e(t) = [\,\rho R^2\, d^2R/dt^2 + 2\rho R(dR/dt)^2]/r - [\,0.5\rho R^4(dR/dt)^2/r^4] . \tag{19}$$

where p(r,t) is the pressure in the liquid at radial coordinate r and time t; R is the bubble radius; and $P_e(t)$ is the pressure inside the vortex core local to the bubble at time t. It is noted that on the bubble surface where r = R, Equation (19) reduces to Equation (1) when p(R,t) denotes the pressure in the liquid just outside the bubble surface.

6

At a sufficiently great distance from the cavity, r>>R, the second term on the right hand side of Equation (19) is negligible. The acoustic pressure $Pa = p(r,t) - P_e (t)$ can be expressed by

$$Pa = \rho R \ [R \ d^2R /dt^2 + 2(dR/dt)^2]/r = \rho/4\pi r[d^2\upsilon /dt^2] \ , \tag{20}$$

where $\upsilon = 4\pi R^3/3$, denotes the volume of the bubble. Equation (20) is the well-known acoustic pressure formula, which states that the acoustic pressure is related to the second time derivative of volume change and the inverse of the distance from the noise source.

Peak Acoustic Amplitude: A sketch of an acoustic spectrum is shown in Figure 2. It is well known (Knapp et al [1970]) that the peak amplitude of noise spectrum is related to the maximum bubble radius, R_{max}. Let Pa_{peak} denotes the peak acoustic amplitude at $R = R_{max}$. We have

$$dR/dt = 0 \qquad at \qquad R = R_{max.} \tag{21}$$

Substitute Equation (21) into Equation (20), we obtain

$$Pa_{peak} = \ \rho R_{max}^2 \ d^2R /dt^2 /r \ . \tag{22}$$

At $R = R_{max}$, $dR/dt = 0$ and Equation (19) gives

$$d^2R /dt^2 = (1/R_{max}) \ (p_v + p_g - P_e - 2S/R)/ \ \rho \ . \tag{23}$$

From Equations (22) and (23), the peak acoustic amplitude can be expressed by

$$Pa_{peak} \ = \ (R_{max} / r) \ (p_v + p_g - P_e(R_{max}) - 2S/R_{max})$$

$$= (R_{max} / r) \ (p(R_{max}) - P_e(R_{max})) \ . \tag{24}$$

If the shapes of the acoustic spectra due to bubble cavitation are similar between the model and full-scale, scaling of the acoustic amplitude can be expressed by

$$Pa_f / Pa_m = Pa_{peak \ f} / Pa_{peak \ m}$$

$$= (R_{max \ f}/R_{max \ m})(r_m / r_f) \ [p(R_{max}) - P_e(R_{max})]_f /[p(R_{max}) - P_e(R_{max})]_m \ . \tag{25}$$

Another approach to derive Equation (25) is by dimensional analysis as discussed by Strasberg [1977]. We know that the intensity of acoustic pressure is inversely proportional to the distance from the noise source. We need a characteristic length scale to normalize the distance: that length scale is the maximum radius. We need a characteristic pressure to normalize the acoustic pressure: that pressure scale is the driving pressure, $p(R) - P_e$, responsible for bubble growth and collapse.

7

Recall that

$$R_{max\,m} / R_{max\,f} = (Re_f / Re_m)^{n/2} / \lambda . \qquad (11)$$

and

$$[p(R_{max}) - P_e(R_{max})]_f / [p(R_{max}) - P_e(R_{max})]_m = (Re_f / Re_m)^n (V_{\infty f}/V_{\infty m})^2 . \qquad (16)$$

From Equations (11), (16) and (25), we obtain the amplitude scaling as follows :

$$Pa_f / Pa_m = [\lambda (Re_f / Re_m)^{-n/2}] (r_m / r_f) [Re_f / Re_m)^n (V_{\infty f}/V_{\infty m})^2]$$

$$= \lambda (Re_f / Re_m)^{n/2} (r_m / r_f) (V_{\infty f}/V_{\infty m})^2 . \qquad (26)$$

The analysis so far has assumed that similar frequency bands will be used for both model and prototype. Following Strasberg's approach, the relationship between noise levels L_f and L_m for prototype and model is

$$L_f = L_m + 20 \, Log \, \lambda + 10 \, Log \, (Re_f/Re_m)^n + 20 \, Log \, (r_m /r_f) + 20 \, Log \, (V_{\infty f}/V_{\infty m})^2 . \qquad (27)$$

The analysis so far is related to a single cavitation bubble. In case there are multiple events of bubble cavitation, Equation (27) can be modified to include multiple events as long as the events are incoherent and the pressures from all signals add up. Let N denote the number of cavitation events per unit time. We have

$$L_f = L_m + 20 \, Log \, \lambda + 10 \, Log \, (Re_f/Re_m)^n + 20 \, Log \, (r_m /r_f)$$

$$+ 20 \, Log \, (V_{\infty f}/V_{\infty m})^2 + 10 \, Log \, (N_f/N_m) . \qquad (28)$$

Comparison with Strasberg Noise Level Scaling: Using dimensional analysis, Strasberg has derived a noise level scaling as follow. Let D denote a length scale such as a propeller diameter, and P_∞ the ambient pressure. He has obtained the non-dimensional π parameter,

$$\pi = (Pa/P_\infty)(r/D)$$

or

$$Pa_f / Pa_m = (D_f / D_m)(r_m / r_f) (P_{\infty f}/ P_{\infty m}) . \qquad (29)$$

A comparison of Equations (25) and (29) shows that amplitude scaling given in Equation (29) by Strasberg and Equation (26) by the present derivation will be the identical if

$$(D_f / D_m) = R_{max\,f}/ R_{max\,m} . \qquad (30a)$$

and

$$(P_{\infty f}/ P_{\infty m}) = (p(R) - P_e)_f / (p(R) - P_e)_m . \qquad (30b)$$

8

Equations (30a) and (30b) show that in the dimensional analysis, if the maximum bubble radius is used as the characteristic length; and the driving pressure inside the vortex core is used to normalize the acoustic pressure, then the present scaling and Strasberg's scaling on acoustic amplitude are identical.

CAVITATION NUMBER SCALING

The present theoretical derivation is based on a similarity flow approach. This means that pressure fields and cavitation patterns in vortex cores are similar between full-scale and model. This similarity requirement is satisfied by setting

$$\sigma_f / \sigma_m \equiv (P_{atm} + \rho g h - p_v)_f / (P_{atm} + \rho g h - p_v)_m = (Re_f / Re_m)^n , \qquad (31)$$

where P_{atm} denotes the atmospheric pressure on the water surface and h denotes the depth of submergence. Since, $p_v \ll P_{atm}$ and $\rho_f \approx \rho_m = \rho$, we have

$$h_f = [(P_{atm} + \rho g h_m)(Re_f / Re_m)^n - P_{atm})] / \rho g . \qquad (32)$$

Equation (32) states that frequency and amplitude scaling of acoustic spectrum measured at a water depth, h_m, are to be applied to full-scale by Equations (17) and (28) at the full-scale depth h_f given by Equation (32).

NUMERICAL VALIDATION OF THE ACOUSTIC SPECTRA SCALING

Two geometrically similar propellers of different sizes are considered [see Figure 1]. The two propellers have $Rp = 61$ cm and 244 cm, respectively. The small propeller is termed model propeller and the large propeller is termed full-scale propeller in this numerical study. The geometric scale ratio λ of these two propellers is $\lambda = 4$. In the present numerical study, the upstream velocity is assumed to be the same for both full-scale and model, $V_{\infty f} = V_{\infty m}$. The axial velocity in the vortex core is assumed to be 13 m/s for both full-scale and model. The assumption of equal axial velocity between full-scale and model is reasonable.

Vortex core size a_c, circulation Γ and tangential velocity distributions V_t along the x-axis on a trailing vortex has been measured with LDV in 36-inch water tunnel on an open propeller (Judge et al [2001]). Using the scaling formula discussed in a paper by Shen et al [2001], the 36-inch water tunnel data are scaled to the model propeller used in this numerical study and given in Figure 5. The pressure distributions are computed by using the Rankine vortex model. The hydrodynamic data on the full-scale propeller are given in Figure 6 by applying McCormick's hypothesis

$$\sigma_f / \sigma_m = - C_{pf} / - C_{pm} = (Re_f / Re_m)^n . \qquad (33)$$

In the present numerical study, we use $n = 0.4$ and the same kinematic viscosity of water for model and full-scale.

9

Acoustic spectrums due to bubble growth and collapse in a trailing vortex core are numerically computed to compare with the scaling formula derived from a similarity flow approaches as shown in the above equations.

Bubble Dynamic Model

It is assumed that the bubble entering the vortex core remains spherical throughout the cavitation process. Bubble dynamics in the cavitation process can be computed by the SAP modified Rayleigh-Plesset Equation (Hsiao et al [2000])

$$R \, (d^2R/dt^2) + 3/2 \, (dR/dt)^2 = 1/\rho \, (p_v + p_g - P_e - 2S/R - 4\mu(dR/dt)/R) + \rho(\bar{U} - \bar{U}_b)^2/4), \quad (34)$$

where $\bar{U} - \bar{U}_b$ denotes the slip velocity between the fluid and the bubble. The viscosity effect in Rayleigh-Plesset Equation is also included in Equation (34), which is used in the present numerical calculations. By taking the Fourier transform of the radiated acoustic pressure Pa given in Equation (20), the acoustic spectra can be obtained.

Numerical results: A small portion of numerical computations is provided in this report for discussions. The history of bubble growth and collapse for the model and full-scale conditions are given in Figures 7 and 8 for the initial bubble size of $R_0 = 5$ µm. Consider first the model case of Figure 7. At $\sigma_m = 7.50$ (upper figure), the 5 µm bubble only experiences marginal growth as the bubble is convected downstream with very small change in acoustic pressure. As the ambient pressure is slightly reduced to $\sigma_m = 7.49$ (lower figure), the bubble grows to a maximum size of $R_{max} = 195$ µm at time t around 0.0081 sec. The bubble then enters a high- pressure zone and the bubble begins to collapse and rebound. The acoustic pressure initially rises above the background level of zero then drops to negative as the bubble grows to a maximum size. The acoustic pressure rises to positive as the bubble begins to collapse. A sharp rise in acoustic pressure is computed when the bubble size reaches the minimum. Since compressibility due to the presence of un-dissolved gas inside the bubble is included in this bubble dynamic model, the minimum bubble size at the collapse is finite. This follows growth and rebound as shown in Figure 7. The qualitative description of rise and fall of acoustic pressure in response to bubble growth and collapse is in agreement with the results given in Fitzpatrick and Strasberg paper [1958]. Note that at time t = 0, the bubble is located at the propeller blade tip. The history of pressure P_e in the vortex core to be encountered by the bubble and the change in gas pressure p_g inside the bubble are also shown in Figures 7 and 8.

Next consider the full-scale case of Figure 8 for the initial bubble size of 5 µm. Due to Reynolds scale effect on vortex core pressure distributions, cavitation inception occur at $\sigma_f = 13.09$. The rise and fall of acoustic pressure in response to bubble growth and collapse along the trailing vortex show the same patterns in the full-scale and in the model.

Scaling of Maximum Bubble Radius

Numerical Results: The maximum bubble radius R_{max} vs normalized cavitation number σ is shown in Figures 9 and 10 for the initial bubble radii of 5 and 10 µm, respectively. The cavitation numbers are normalized by $(Re_m / Re)^{0.4}$, where $Re = Re_m$ for the model scale curve

10

and Re = Re_f for the full-scale curve. Cavitation inception occurs around the normalized cavitation numbers of 7.50 and 7.52. Once the cavitation is beyond inception ($\sigma < 7.5$), the maximum bubble size increase sharply and almost linearly with the reduction of cavitation number. Instead of R_{max}, we can plot $R_{max\ f}\ /\ R_{max\ m}$ vs normalized σ as shown in Figure 11. Except in the neighborhood of cavitation inception region, the bubble dynamic calculations give the ratio of

$$R_{max\ f}\ /\ R_{max\ m} \approx 3.0 . \tag{35a}$$

Present Similarity flow method: The ratio of maximum bubble radius derived from similarity flow approach is given in Equations (10) and (11):

$$R_{max\ f}/\ R_{max\ m} = a_{cf}\ /\ a_{cm} = \lambda\ (Re_f\ /\ Re_m\ )^{-0.2} = 4^{0.8} = 3.03 . \tag{35b}$$

This value of 3.03 derived from similarity flow approach is in very good agreement with the value 3.0 obtained from bubble dynamics numerical calculations. The good agreement between similarity flow method [Equation (35b)] and numerical calculations [Equation (35a)] supports the assumption used in dimensional analysis that the characteristic length to normalize the maximum bubble size is the vortex core radius [Equation (10)], not a propeller diameter or a blade chord length.

Scaling of Frequency at Peak Amplitude of Acoustic Spectrum

The acoustic pressure is computed from Equation (20). The acoustic amplitude spectrum is computed from the following equation.

$$s = \left| \int_0^\infty Pa\ e^{-i\omega t} dt \right| / 2\pi \tag{36}$$

Acoustic spectra have been calculated for several initial bubble radii and cavitation numbers. As an example, the spectra expressed in a narrow band analysis are shown in Figure 12 with the initial bubble radius of 10 μm at $\sigma = 7.2$ for the model and $\sigma = 7.2 \times (4)^{0.4} = 12.53$ for the full-scale, respectively. In the plots, the notation $D = 0.5\ a_c$ denotes that the 10 μm bubble is released at half radial distance from vortex core center to the edge of the vortex core. The bubble is released at the upstream location of $x = 0$, corresponding to the blade tip location. Discussion of the dynamic process of a bubble spiraled into the vortex center can be found in the report by Hsiao et al [2000]. Another example is given in Figure 13 for the initial bubble radius of 2.5 μm at $\sigma = 7.15$ for the model and $\sigma = 7.15 \times (4)^{0.4} = 12.45$ for the full-scale, respectively.

Numerical results: Figures 12 and 13 give the frequency at peak amplitude to be around $f_{pf} \approx 900$ Hz for the full-scale spectrum and $f_{pm} \approx 2110$ Hz for the model spectrum for both 10 and 2.5 μm bubbles. Both full-scale and model frequencies are relatively low when compared with some of the water tunnel measurements. This is because, we only consider cases where the maximum pressure peak occurs at R_{max}. It is remarked that the peak frequency depends on the vortex core size and the encounter pressure. The peak frequency can be changed if these two parameters are changed. Numerical calculations give

11

$$f_{pf} = f_{pm} (900 / 2110) = f_{pm} / 2.34 .$$ (37a)

This numerical result is quite different from Strasberg's classic λ scaling. Note that the linear scale ratio used in this study is $\lambda = 4$.

Present Similarity flow method: Equation (17) gives the scaling formula by

$$f_{pf} = f_{pm} \left(\frac{1}{\lambda}\right)\left(\frac{Re_f}{Re_m}\right)^n\left(\frac{V_{\infty f}}{V_{\infty m}}\right) = f_{pm} \left(\frac{1}{4}\right)(4)^{0.4} = f_{pm}\left(\frac{1}{4}\right)^{0.6} = f_{pm} / 2.30$$ (37b)

Note that $V_{\infty f} = V_{\infty m}$, $v_f = v_m$, $\lambda = 4$, and $n = 0.4$ are used in this numerical study.

The good agreement between the similarity flow method [Equation (37b)] and the numerical calculations [Equation (37a)] supports the assumption used in dimensional analysis that the characteristic length and pressure term to normalize the peak frequency are maximum bubble radius and encounter pressure in the vortex core. All other calculations not shown in this report give the same good agreement between frequency scaling of Equation (17) and bubble dynamic calculations.

Numerical calculations show that for a given cavitation number, all bubbles of different initial radii grow to about the same maximum bubble radius R_{max}. This is an intrinsic property of the bubble dynamic equation. This means that frequency-scaling formula given in Equation (17) holds regardless of the initial bubble size in the free stream.

Scaling of Peak Amplitude of Acoustic Spectrum

Numerical Results: Figure 12 gives the model and full-scale amplitude spectra for the initial bubble radius of $R_0 = 10$ µm. The computed peak amplitudes for the full-scale and model spectra are $p_f \approx 2.5 \times 10^{-2}$ Pa and $p_m \approx 4.5 \times 10^{-3}$ Pa for the model, respectively. The distances between the hydrophone location and the cavitation bubble used in these calculations are $r_f = 0.52$ m for the full-scale and $r_m = 0.32$ m for the model.

Figure 13 gives the model and full-scale amplitude spectra for the initial bubble radius of $R_0 = 2.5$ µm. The peak amplitudes for the full-scale and model spectra are $p_f \approx 7.0 \times 10^{-2}$ Pa and $p_m \approx 1.4 \times 10^{-2}$ Pa for the model, respectively. The distances between the hydrophone location and the cavitation bubble are $r_f = 0.52$ m for the full-scale and $r_m = 0.32$ m for the model.

Let L_f and L_m denotes the noise level generated by the cavitation bubble for the full-scale and model, respectively. The differences in noise level between full-scale and model for $R_0 = 10$ and 2.5 µm are given by

$$\Delta L = L_f - L_m = 20 \, Log \, (p_f / p_m)$$

$$= 20 \, Log \, (2.5 \times 10^{-2} / 4.5 \times 10^{-3}) = 14.9 \, dB \quad \text{for } R_0 = 10 \text{ µm}$$ (38a)

$$= 20 \, Log \, (7.0 \times 10^{-2} / 1.4 \times 10^{-2}) = 14.0 \, dB \quad \text{for } R_0 = 2.5 \text{ µm.}$$ (38b)

Present Similarity flow method: The amplitude scaling is given in Equation (28) as follows

$$\Delta L = L_f - L_m = 20 \, Log \, \lambda + 10 \, Log \, (Re_f / Re_m)^n + 20 \, Log \, (r_m / r_f)$$

$$+ \, 20 \, Log \, (V_{\infty f} / V_{\infty m})^2 + 10 \, Log \, (N_f / N_m)$$

$$= 20 \, Log \, 4 + 10 \, Log \, (4)^{0.4} + 20 \, Log \, (0.32 / 0.52) = 10.3 \, dB. \tag{38c}$$

Note $N_f = N_m = 1$ for a single bubble study.

A comparison of numerical calculations and amplitude scaling formula given in Equations (38a), (38b) and (38c) indicates a difference of 3.7 dB for $R_0 = 2.5$ μm and 4.6 dB for $R_0 = 10$ μm. Analysis of the numerical data indicates that the cavitation bubble experiences growth and collapse at slightly different normalized encounter pressure between the model and full-scale. This slight difference in encounter pressure has very minor effect on frequency but some effect on acoustic amplitude. Further study is needed to quantify the initial bubble size effect on acoustic amplitude. At present, Equation (28) is considered to be valid in a global sense with uncertainty of a few dB.

CONCLUSIONS

Scaling of noise generation due to bubble cavitation in a trailing vortex has been theoretically investigated. Three scaling formulas have been derived based on geometric, kinematic and dynamic similarities between full-scale and model. The first two scaling formulas provide frequency and noise level (amplitude) scaling to obtain full-scale spectrum from model measurements. The third cavitation number scaling relates the depths or speeds between full-scale and model for application of the acoustic scaling.

Due to Reynolds scaling effects on vortex core dynamics and pressure distributions in a trailing vortex, the present frequency scaling is noticeably different from Strasberg's classic λ scaling. However, if viscous effects are not considered, the present theory gives the same frequency scaling as Strasberg's λ scaling. The present frequency scaling represents a Reynolds scaling correction of Strasberg's λ scaling.

The frequency scaling is found to be insensitive to nuclei sizes.

The present noise level (amplitude) scaling also represents a Reynolds scaling correction of Strasberg's noise level scaling. If viscous effects are not considered, the present noise level scaling agrees with Strasberg's noise level scaling.

Acoustic narrow band spectrums generated by a spherical cavitation bubble are numerically studied by using a bubble dynamic computer code developed by Dynaflow Inc. Frequency scaling formula derived from similarity flow approach is shown to be in excellent agreement with bubble dynamic calculations.

13

Noise level (amplitude) scaling formula derived from similarity flow approach is found to differ 3.7 dB for $R_0 = 2.5$ μm and 4.6 dB for $R_0 = 10$ μm from bubble dynamic calculations.

Further numerical studies are needed to quantify nuclei size effect on noise level scaling.
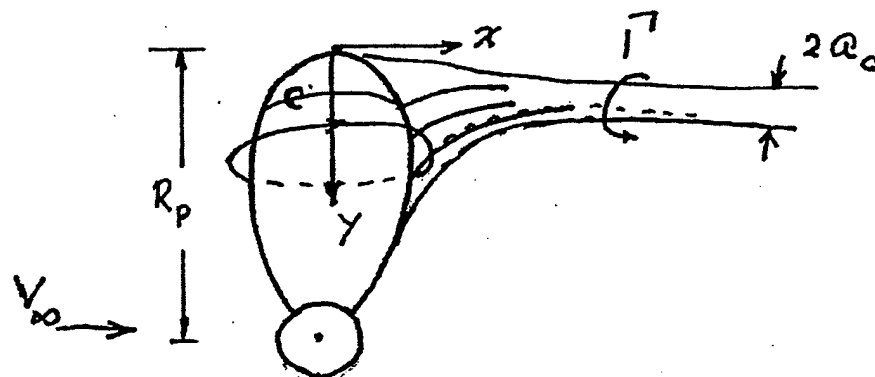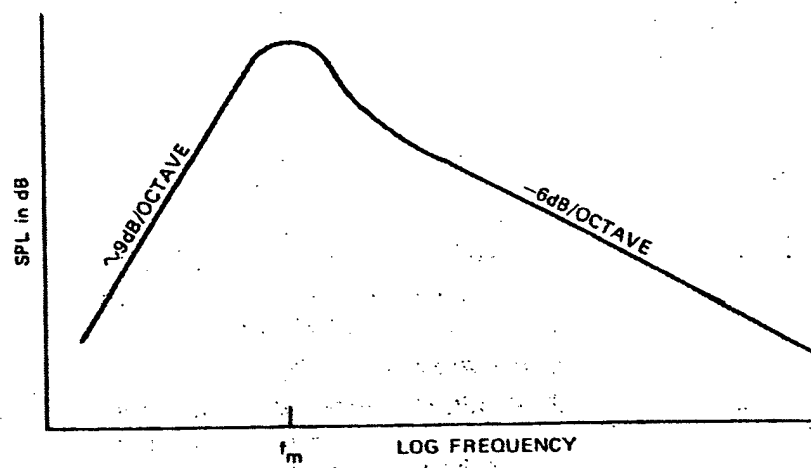
ACKNOWLEDGEMENTS

14

Figure 1. Sketch of a Trailing Vortex

Figure 2. Idealized Cavitation Spectrum (Ross 1976)
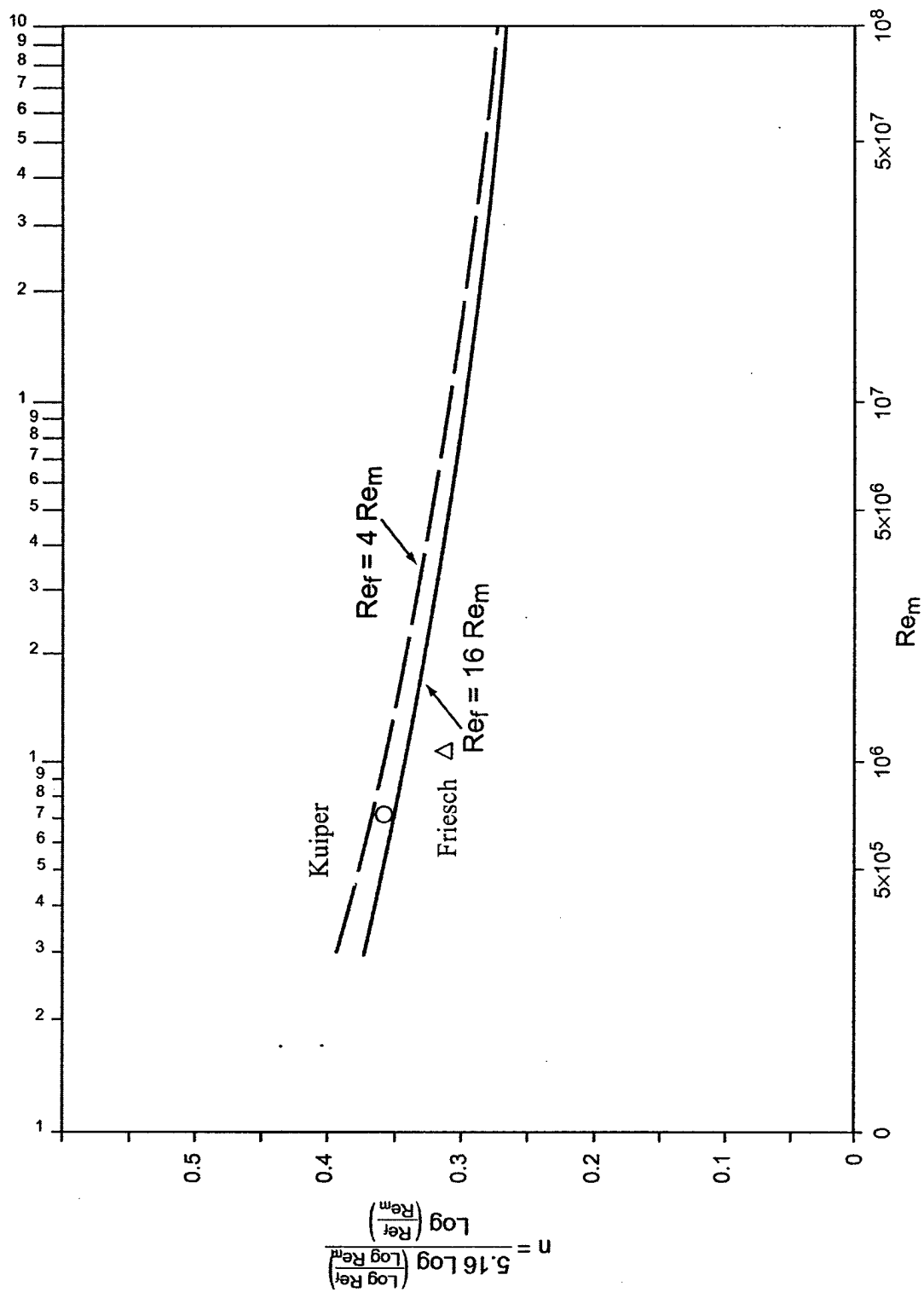
Figure 3. The Values of n Computed vs. Measured

Figure 4. The Values of n for 1/4-scale and 1/16-scale Models

$$n = \frac{5.16 \, \text{Log} \left(\frac{\text{Log Re}_f}{\text{Log Re}_m} \right)}{\text{Log} \left(\frac{\text{Re}_f}{\text{Re}_m} \right)}$$

Model Scale Rp=60.96cm U=13m/s Lamb Model is used				
X (m)	a (mm)	Γ (m^2/s)	vt (m/s)	-Cp
0.000	0.792	0.000	0.000	0.000
0.107	1.366	0.232	19.344	7.542
0.146	1.597	0.252	17.979	6.515
0.241	1.890	0.257	15.470	4.824
0.511	2.652	0.354	15.210	4.663

Figure 5. Pressure Distributions in the Vortex Core used in the Present Numerical Calculations : Model

18

Full Scale Rp=243.84cm U=13m/s Lamb Model is used				
X (m)	a (mm)	Γ (m^2/s)	vt (m/s)	-Cp
0.000	2.402	0.000	0.000	0.000
0.429	4.139	0.928	25.509	13.115
0.583	4.842	1.008	23.689	11.311
0.966	5.729	1.028	20.418	8.403
2.043	8.039	1.416	20.043	8.097

Figure 6.   Pressure Distributions in the Vortex Core used
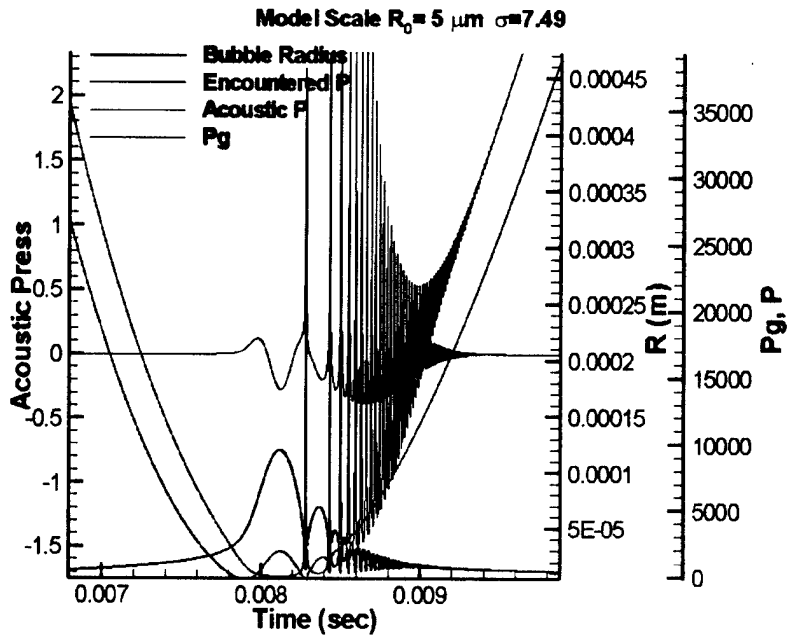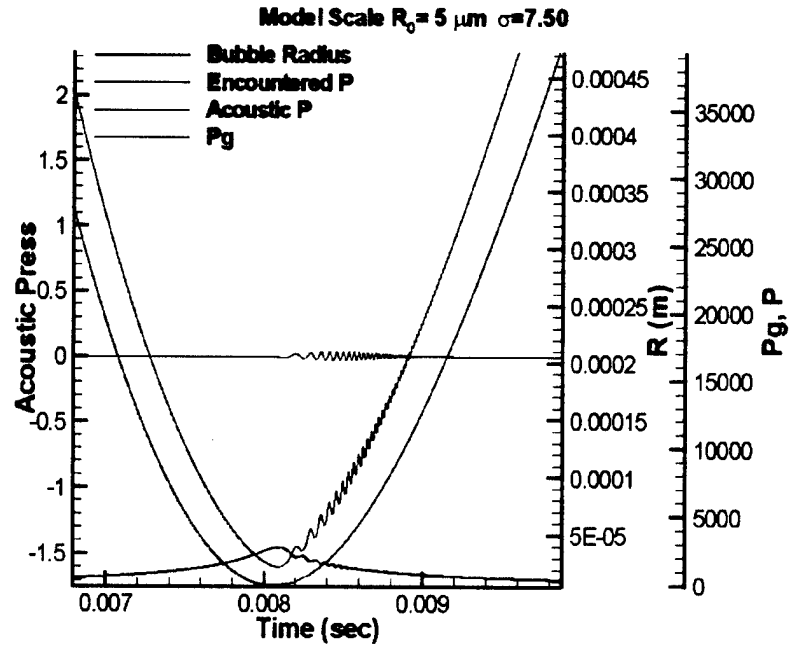in the Present Numerical Calculations : Full-Scale

19

Figure 7. Computed Bubble Radius History, Gas Pressure, Encountered Pressure and Radiated Acoustic Pressure at $R_0 = 5$ μm and σ = 7.50 and 7.49 for Model Scale
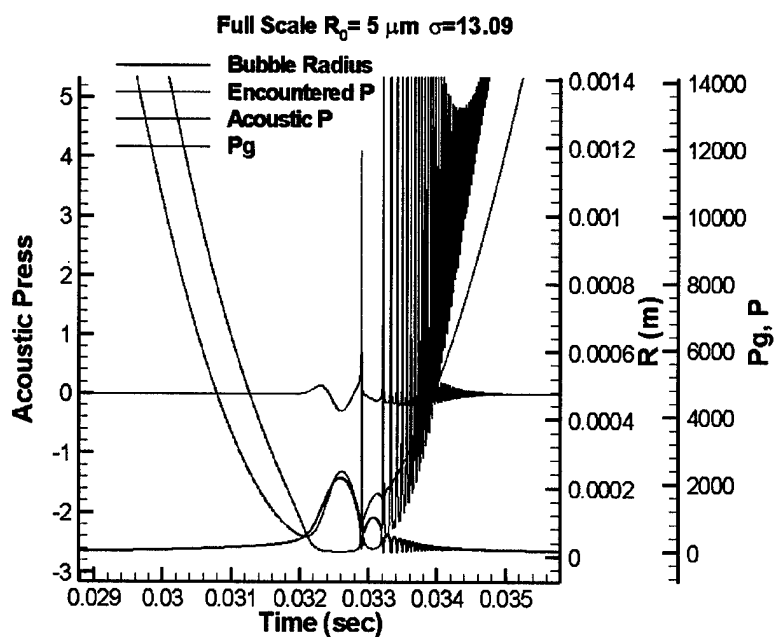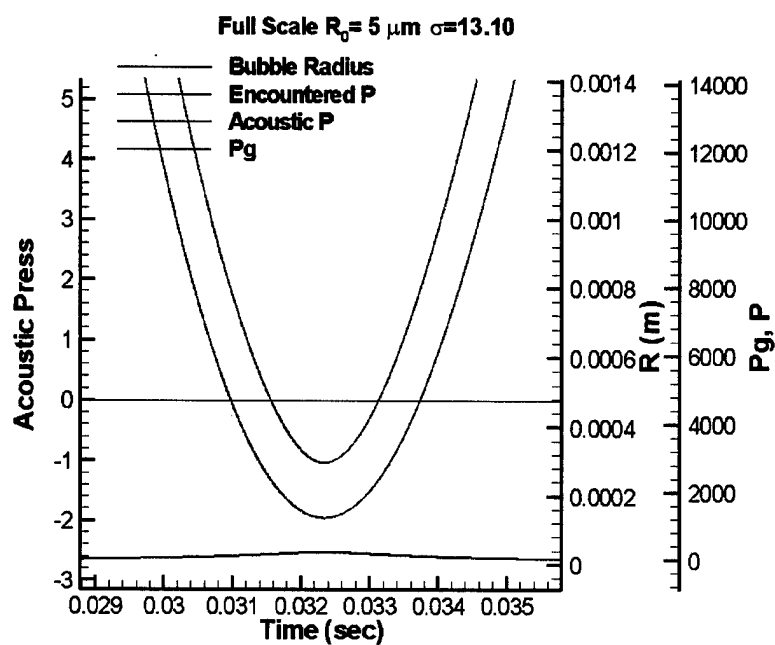
Figure 8. Computed Bubble Radius History, Gas Pressure, Encountered Pressure and Radiated Acoustic Pressure at $R_0 = 5$ µm and $\sigma = 13.10$ and 13.09 for Full-Scale
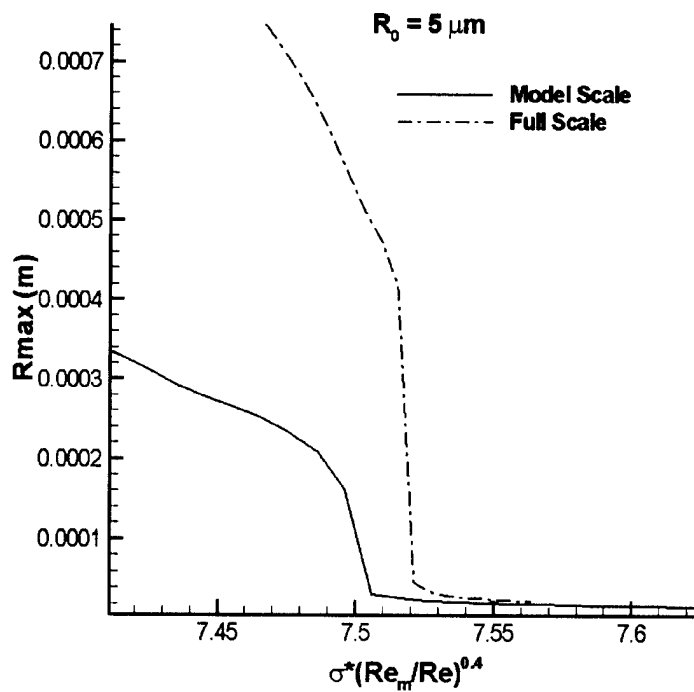
Figure 9. Maximum Bubble Size versus Normalized Cavitation Number
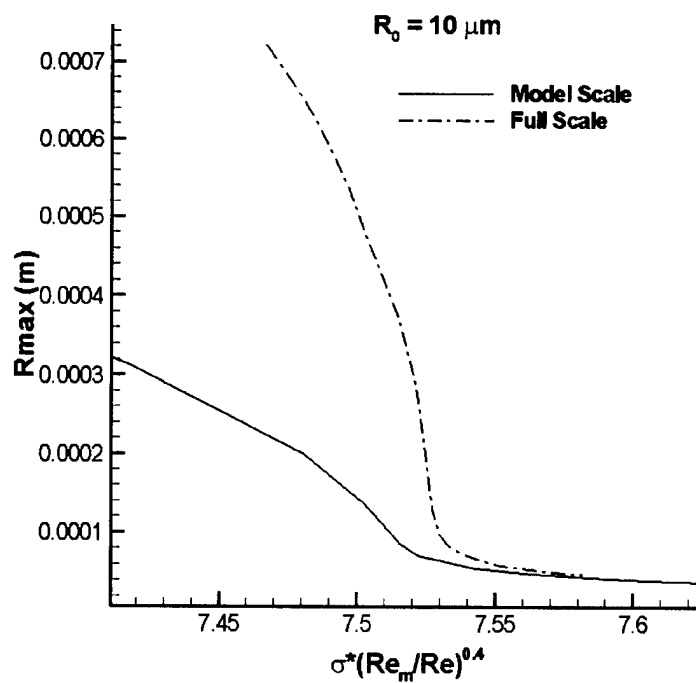for Full-Scale and Model with $R_0 = 5$ μm

Figure 10. Maximum Bubble Size versus Normalized Cavitation Number
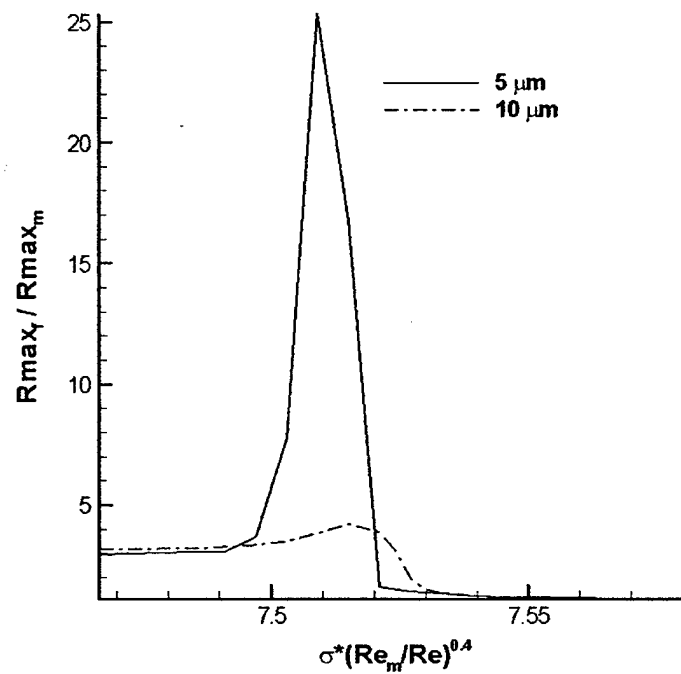for Full-Scale and Model with $R_0 = 10$ μm

Figure 11. $R_{max\ f} / R_{max\ m}$ vs. σ
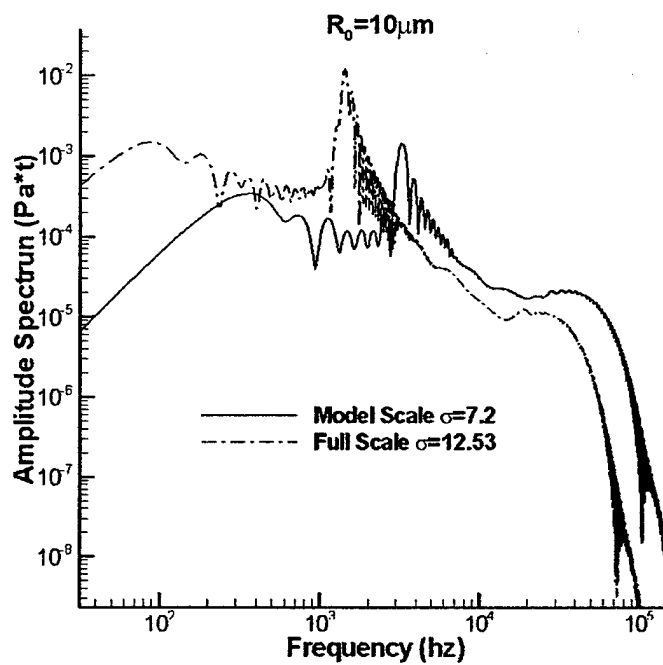

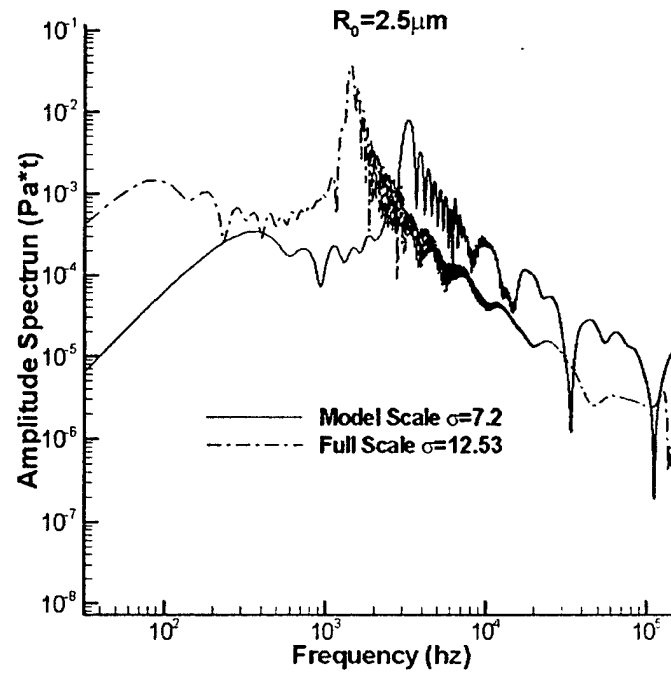Figure 12. Numerically Computed Acoustic Spectra for
Initial Bubble Size of $R_0 = 10$ μm

Figure 13. Numerically Computed Acoustic Spectra for
Initial Bubble Size of $R_0 = 2.5$ μm

REFERENCES

Acosta A. J. and B. R. Parkin, 1975, "Cavitation Inception – A Selective Review," Journal of Ship Research, Vol. 19, No. 4

Baiter, H-J, 1982, "Estimates Of The Acoustic Efficiency Of Collapsing Bubbles," International Symposium on Cavitation Noise, The Winter Annual Meeting, ASME, Phoenix, Arizona

Baiter, H-J, 1989, "On Cavitation Noise Scaling With The Implication Of Dissimilarity In Cavitation Inception," International Symposium on Cavitation Noise and Erosion in Fluid Systems, ASME Winter Annual Meeting, San Francisco, California

Blake, W. K. and M. M. Sevik, 1982, "Recent Developments In Cavitation Noise Research," International Symposium on Cavitation Noise, The Winter Annual Meeting, ASME, Phoenix, Arizona

Blake, W. K., 1986, "Propeller Cavitation Noise: The Problems Of Scaling And Prediction," International Symposium on Cavitation and Multiphase Flow Noise, ASME FED-Volume 45

Chahine, G. L., 1979, "Etude Locale du Phenomene de Cavitation – Analyse des Facteurs Regissant la Dynamique des Interfaces," Doctorat D'Etat Es-Science Thesis, Universite Pierre et Marie Curie

Chahine, G. L. and Y. T. Shen, 1986, "Bubble Dynamics And Cavitation Inception In Cavitation Susceptibility Meters," Journal of Fluids Engineering, Volume 108

Fitzpatrick, H. and M. Strasberg, 1956, "Hydrodynamic Source Of Sound," 1st Symposium on Naval Hydrodynamics, Washington D. C.

Fitzpatrick, H., 1958, "Cavitation Noise," 2nd Symposium on Naval Hydrodynamics, Washington D. C.

Freisch J. and C. Johannsen, 1995, "Study On Tip Vortex Cavitation Inception For Navy Propellers," International Symposium on Cavitation, CAV 1995, Deauville, France

Hsiao, C-T, G. L. Chahine and H. L. Liu, 2000, "Scaling Effects On Bubble Dynamics In A Tip Vortex Flow: Prediction Of Cavitation Inception And Noise," Dynaflow Inc, Report 98007-1NSWC

Hsiao, C-T and G. L. Chahine, 2002, "Prediction Of Vortex Cavitation Inception Using Coupled Spherical And Non-Spherical Models And UnRANS Computations," 24th ONR Symposium, Fukuoka, Japan

Judge, C., G. Oweis, S. Ceccio, S. Jessup, C. Chesnakas and D. Fry, 2001, "Tip-Leakage Vortex Inception On A Ducted Rotor," 4th Int. Symp. on Cavitation CAV 2001

Knapp R. T., J. W. Daily and F. G. Hammitt, 1970, "Cavitation", McGraw-Hill Book Company.

Lamb, H., 1945, "Hydrodynamics," Dover Publication, 1st American Edition

McCormick, B.W., 1954, "A Study Of The Minimum Pressure In A Trailing Vortex System," PhD Dissertation, Penn State University

McCormick, B.W., 1962, "On Cavitation Produced By A Vortex Trailing From A Lifting Surface," Journal of Basic Engineering

REFERENCES – Continued

Plesset M. S., 1948, "Dynamics Of Cavitation Bubbles," Journal of Applied Mechanics

Ross D., 1976, "Mechanics of Underwater Noise," Permagon Press, Oxford

Shen, Y.T., G. L. Chahine, C-T Hsiao, S. Jessup, 2001, "Effects of Model Size and Free-Stream Nuclei on Tip Vortex Cavitation Scaling," 4th Int. Symp. on Cavitation CAV 2001

Shen Y. T., S. Jessup, and S. Gowing, 2001, "Tip Vortex Cavitation Inception Logarithmic Scaling," NSWCCD-50-TR-2001/060 Report

Strasberg, M., 1956, "Gas Bubbles As Sources Of Sound In Liquids," J.A.S.A. 28

Strasberg, M., 1957, "The Influence Of Air-Filled Nuclei On Cavitation Inception," David Taylor Model Basin Report 1078

Strasberg, M. (1977), "Propeller Cavitation Noise After 35 Years Of Study," Proceeding ASME Symposium on Noise and Fluids Engineering, Atlanta, Ga.

INITIAL REPORT DISTRUBITION

Organization	Name	Copies
Dynaflow, Inc.	Chahine, G.	1
	Hsiao C.	1
Mississippi State	Whitfield	1
NAVSEA		
93R	Dalmer, D.	1
	Stout, M.	1
NSWCCD		
Code 0114	Kim, K-H	1
Code 3421	NSWCCD Library	1
Code 50	Webster, B.	1
Code 506	Walden, D.	2
Code 5080	Boswell, R.	1
	Brown, J.	1
	Cox, B.	1
	Cross, R.	1
	Lee, J.	1
	Meyer, R.	1
Code 5200	Day, W.	1
	Stenson, R.	1
Code 5400	Chen, B.	1
	Etter, R.	1
	Gorski, J.	1
	Jessup, S.	1
	Remmers, K.	1
	Shen, Y.	5
	Szwerc, R.	1
	Wilson, M.	1
Code 5500	Applebee, T.	1
Code 5600	Koh, I.	1
Code 70	Blake, W.	1
	Strasberg, M.	1
Code 725	Shang, P.	1
	Gonzales, J.	1
DTIC		2
PSU/ARL	Billet, M.	1
	Straka, W.	1
University of Michigan	Ceccio, S.	1
University of Minnesota	Arndt, R.	1